

Cite this: DOI: 10.1039/c0xx00000x

www.rsc.org/xxxxxx

ARTICLE TYPE

## Quantification of mRNA in living cells by double-stranded locked nucleic acid probes

Reza Riahi,<sup>a</sup> Zachary Dean,<sup>b</sup> Ting-Hsiang Wu,<sup>c</sup> Michael A. Teitell,<sup>d</sup> Pei-Yu Chiou,<sup>c</sup> Donna D. Zhang,<sup>ef</sup> and Pak Kin Wong<sup>\*af</sup>

<sup>5</sup> Received (in XXX, XXX) Xth XXXXXXXXX 20XX, Accepted Xth XXXXXXXXX 20XX

DOI: 10.1039/b000000x

Double-stranded probes are homogeneous biosensors for rapid detection of specific nucleotide sequences. These double-stranded probes have been applied in various molecular sensing applications, such as detection of bacterial 16S rRNA and real-time polymerase chain reaction. In this study, we present the design and optimization of double-stranded probes for single-cell gene expression analysis in living cells. The probes can be delivered to a large number of cells simultaneously by cationic liposomal transfection or to individual cells selectively by photothermal delivery. With alternating DNA/LNA monomers for optimizing the stability and specificity, we show that the probe is stable in living cells for over 72 hours post-transfection and is capable of detecting changes in gene expression induced by external stimuli. We also demonstrate that the probe quantifies intracellular mRNA in living cells through the use of an equilibrium analysis. With its effectiveness and performance, the double-stranded probe represents a broadly applicable approach for large-scale single-cell gene expression analysis toward numerous biomedical applications, such as systems biology, cancer recognition, and drug screening.

### Introduction

The investigation of complex biological processes, such as tissue morphogenesis, collective cell migration, and gene regulatory networks, can be benefited tremendously by novel biosensing techniques with high spatiotemporal resolution.<sup>1</sup> In particular, molecular probes with qualities including high stability, sensitivity and specificity are highly sought-after for long-term monitoring of gene expression in individual cells. Investigating the dynamic regulation of gene expression, for instance, requires single cell analysis techniques to monitor the dynamics of cellular responses. While single-cell polymerase chain reaction and high throughput microfluidic analysis are available to measure gene expression down to the single cell level,<sup>2,3</sup> the requirement of cell lysis prior to measurement introduces challenges in analyzing the dynamics and spatial distribution of genes for a large number of cells. Thus, innovative biosensing techniques are required to address these challenges in investigating complex biological systems.

Molecular beacon, as an example, has been developed for gene expression analyses in living cells and has been broadly utilized in various biological applications.<sup>4-10</sup> A molecular beacon is a short hairpin oligonucleotide that binds to a specific target oligonucleotide sequence and produces a fluorescent signal. For intracellular detection, the stability of molecular beacons is a major consideration particularly when they are employed in long-term gene expression monitoring. DNA sequences encompassing molecular beacon probes are vulnerable to nuclease digestion and nonspecific binding by DNA binding proteins. These processes

can in turn generate false-positive signals. To overcome the stability issue, nuclease-resistant nucleic acid monomer such as 2'-O-methyl RNA,<sup>11, 12</sup> peptide nucleic acids (PNA),<sup>13, 14</sup> and locked nucleic acids (LNA)<sup>15, 16</sup> have been incorporated into the molecular beacon design. For instance, LNA and 2'-O-methyl bases have been shown to improve the stability of molecular beacons inside living cells, while retaining similar or better solubility and molecular recognition features to natural DNA. In the case of LNA, alternating DNA/LNA bases has been demonstrated to balance between the binding affinity and the stability of the probes, resulting in enhanced performance for intracellular measurement.<sup>17</sup>

Another homogeneous scheme for sensing specific nucleic acid sequences is the double-stranded probe, which consists of two complementary oligonucleotide sequences labeled with a fluorophore and quencher at the 5' and 3' ends.<sup>18-21</sup> When the probes enter a cell lacking the probe's specific target mRNA, the donor and quencher sequences remain in close proximity, diminishing the fluorescence signal. In the presence of the target mRNA, the quencher sequence is displaced from the donor sequence due to the thermodynamically-driven binding event between the donor and the target sequences (Figure 1a-b). This separation between quencher and donor sequences enables the donor sequence to fluoresce. When compared with molecular beacons, the double-stranded probe has several advantages including the possibility of adjusting the quencher-to-fluorophore ratio for noise minimization as well as the flexibility of modifying the length of the quencher sequence to improve the specificity and kinetics of the assay.<sup>18</sup> The double-stranded probe

has been successfully demonstrated for single base mismatch discrimination,<sup>22</sup> transcription factor detection,<sup>23, 24</sup> quantification bacterial 16S rRNA,<sup>20</sup> and real-time PCR.<sup>24, 25</sup> Nevertheless, several key aspects of the double-stranded probe for intracellular gene expression measurement have not been explored and optimized systematically. In particular, the feasibility of adopting nuclease-resistant building blocks in the double-stranded probe should be evaluated to improve the long-term stability and specificity of the probe in living cells. Furthermore, methods for high throughput delivery to multiple cells simultaneously and selective delivery to individual cells rapidly should be developed for elucidating complex biological processes. The ability and specificity of using double-strand probes for measuring inducible genes should also be evaluated. More importantly, the applicability of the double-stranded probe for the quantification of intracellular mRNA needs to be explored toward systems investigation of biological processes.

In this study, we adopt LNA monomers in the design of double-stranded probes (dsLNA) for monitoring intracellular gene expression at the single cell level. In particular, we design dsLNA probes targeting  $\beta$ -actin, heme oxygenase-1 (HO-1), heat shock protein 70 (HSP70), and a random sequence control by incorporating alternating DNA/LNA bases with a goal of optimizing their stabilities and specificity. The stability of the dsLNA probes are compared with other nucleotide modifications. We also optimize the procedures for transfecting dsLNA with cationic liposomal transfection reagents for detecting the gene expression in a large number of cells concurrently and with photothermal nanoblade to individual cells selectively. To evaluate the ability of dsLNA probes to detect inducible genes, we carry out tert-butylhydroquinone (tBHQ) treatment and temperature elevation studies to induce HO-1 and HSP70 gene expression, respectively. The behaviors of the probe inside living cells are studied systematically by transfecting donor-quencher (DQ) duplex and donor-target (DT) duplex into the cells. By considering an equilibrium analysis, we evaluate the feasibility of quantifying the mRNA concentration in living cells using dsLNA probes.

## Materials and methods

### Probe Design and preparation

A dsLNA probe consists of two oligonucleotide sequences for rapid detection of specific nucleic acid sequences. A donor sequence complementary to a target mRNA is designed and is synthesized with alternating DNA/LNA monomers. The donor sequence is labeled with a fluorophore (6-FAM) located at the 5' end. For homogeneous detection of the target gene, a shorter, alternating DNA/LNA sequence complementary to the donor sequence is designed and labeled with a quencher (Iowa black) at its 3' end. To compare its stability, two other double-stranded probes were designed consisting of DNA only or 2'-O-methyl RNA. All nucleic acid probes and corresponding target sequences in this study were synthesized by Integrated DNA Technologies Inc. Three different probes targeting  $\beta$ -actin, HO-1 and HSP70 mRNAs were designed based on sequences from the NCBI GenBank database (Table 1). A random probe sequence not significantly complementary to any known intracellular

mRNA was designed as a negative control. The specificity of all probes sequences were evaluated by NCBI Blast database (NIH, D.C). Before introducing the probe to the cells, the dsLNA probes were prepared by mixing donor and quencher sequences in a buffer of 10 mM Tris-EDTA and 0.2 M NaCl. After 5 minutes of incubation in a water bath at 95°C, the probes were allowed to slowly cool down to room temperature over the course of 3 hours before they were ready to transfect into cells and detect the gene of interest. A low background noise was achieved at a ratio of 1 donor to 2.5 quencher sequences and was used in this study.<sup>25</sup>

### Cell Culture and transfection of the probe

Human mammary gland adenocarcinoma, MDA-MB-231, was obtained from ATCC (Manassas, VA). Cells were maintained in Dulbecco's modified Eagle's medium (Invitrogen, Carlsbad, CA) supplemented with 10% fetal bovine serum (Sigma, St. Louis, MO), 2 mM HEPES buffer, and antibiotics (0.1% Gentamycin, Sigma). Cells were stored at 37°C in a humidified incubator containing 5% CO<sub>2</sub>. Cells were plated overnight in 24-well plates at an initial concentration of 10<sup>5</sup> cells/ml before transfection. Once reaching 90-95% confluency, cells were transfected with 1.0  $\mu$ g probe at different transfection reagent ratios. Transfection reagents, including Lipofectamine, FuGENE HD, and Lipofectamine 2000 in opti-MEM (Invitrogen, Grand Island, NY) were tested to assess probe transfection efficiency. In other experiments, cells were transfected with Lipofectamine 2000 to measure intracellular gene expression (Figure 1c).

Delivery with the photothermal nanoblade was performed as described.<sup>26, 27</sup> Briefly, a Nd:YAG laser (Minilite I; Continuum) operated at 532 nm wavelength and 6 ns pulsewidth was applied to induce a ultrafast cavitation bubble near a titanium-coated micropipette. The cavitation bubble locally ruptured the cell membrane to allow delivery of the dsLNA probe to the cells with high efficiency and viability. With a liquid delivery system synchronized with the pulsed laser, a volume of ~1 pL of the dsLNA probe solution was delivered to the cells. Bright field and fluorescence images were captured using a Zeiss Axiovert 40CFL inverted fluorescence microscope with a Canon digital camera.

### Inducible gene detection

To examine the ability of dsLNA probe to detect gene expression changes in cells, experiments were performed utilizing either chemical or physical stimuli to upregulate the target gene of interest. In the experiment, cells transfected with dsLNA probes were treated with 50  $\mu$ M tBHQ, a known HO-1 activator, for 16 hours prior to taking measurements.<sup>28</sup> To induce changes of HSP70 mRNA, a heat-responsive gene,<sup>29</sup> the cell culture incubation temperature was increased from 37°C to 42°C for 1.5 hours. The intensity of the HSP70 probe was measured after 5 hours.

### Intracellular probe concentration calibration

To estimate the probe concentration transfected into a cell, we carried out two different experiments using random donor probes hybridized with synthetic targets, i.e., random donor-target (DT) duplex. We first plated cells on a cover slip overnight. Cells were transfected with a random DT duplex and intensity measurements were performed after 12 hours. Since the random

probe sequence has no complementary target gene inside the cell, intracellular signals were primarily due to the DT duplex transfected. In the second experiment, we placed different concentrations of a pre-hybridized random DT duplex between two cover slips. It is known that the height of breast cancer cells is typically  $\sim 5 \mu\text{m}$ .<sup>30</sup> We introduced the random donor-target duplex to create a  $5 \mu\text{m}$ -thick sample of solution between two cover slips. We measured the intensity levels of the random DT duplex at different concentrations to obtain a linear calibration curve to quantify the probe concentration inside a cell. Assuming the average radius of a cell is  $12 \mu\text{m}$ ,<sup>31</sup> we determined the probe concentration transfected into a cell with an average cell volume of  $7240 \mu\text{m}^3$ . The average concentration and number of dsLNA probes in the cells can then be estimated and applied for obtaining the standard curve to quantify intracellular mRNA in living cells.

### Equilibrium Analysis

An equilibrium analysis has been previously demonstrated to describe the probe-target binding dynamics without any fitting parameters.<sup>22</sup> The dsLNA probe can be represented by two coupled reversible binding reactions (equations (1) and (2)).



where  $D$  is the donor probe,  $Q$  is the quencher probe, and  $T$  is the target.  $DQ$  and  $DT$  are the fluorophore–quencher probe and the fluorophore–target duplex. These binding reactions lead to equilibrium constant equations (3) and (4), where  $K_{DQ}$  and  $K_{DT}$  are the equilibrium constants of donor–quencher and donor–target hybridizations respectively. The equilibrium constants depend on the Gibbs free energy change,  $\Delta G$ , associated with the hybridization of the complementary probe sequences. The equilibrium constant can be estimated by  $K = e^{-\Delta G/RT}$  where  $R$  and  $T$  are the gas constant and the temperature respectively. Also, the mass conservation law results in equations (5) and (7), where  $D_0$ ,  $Q_0$ , and  $T_0$  represent the initial concentrations of donor, quencher and target sequences.

$$K_{DQ} = \frac{[DQ]}{[D][Q]} \quad (3)$$

$$K_{DT} = \frac{[DT]}{[D][T]} \quad (4)$$

$$D_0 = [D] + [DQ] + [DT] \quad (5)$$

$$Q_0 = Q \quad (6)$$

$$T_0 = [DT] + [T] \quad (7)$$

In our experiment the concentration of the donor is small in comparison to the concentration of the quencher, i.e.,  $D \ll Q$ ; therefore, we assume that  $Q = Q_0$ . By solving equations (3)–(7), the equilibrium concentrations of the free donor  $[D]$ , the donor–quencher  $[DQ]$ , and the donor–target  $[DT]$  are given by equations (8)–(10).

$$[D] = \frac{-M + \sqrt{M^2 + 4ND_0}}{2N} \quad (8)$$

$$[DQ] = [D]QK_{DQ} \quad (9)$$

$$[DT] = \frac{[D]K_{DT}T_0}{1 + [D]K_{DT}} \quad (10)$$

where  $M = 1 + QK_{DQ} + K_{DT}T_0 - D_0K_{DT}$ , and  $N = K_{DT} + QK_{DQ}K_{DT}$ . At a low background level, the fluorescence signal can be determined by equation (10) according to the target concentrations. It should be noted that the free energy change (and the equilibrium constant) can be directly estimated by Mfold based on the probe sequence and experimental conditions (e.g., salt concentration and temperature).<sup>32</sup> In this study, all three dsLNA probe designs have the same length of donor and quencher sequences (Table 1). In the calculation, we ignored the slight differences in free energy among the probes and predict one calibration curve for the quantitative estimation of the target concentration.

### Imaging and data analysis

Probe intensities were monitored with an inverted fluorescence microscope (TE2000-U, Nikon) and fluorescence images were acquired using a CCD camera (SensiCamQE, Cook corp.) at different time points. All images were taken with a 1.0 second exposure time under the same conditions (e.g., fluorescent excitation intensity and temperature) in order to compare the relative fluorescence intensity. Data collection and imaging analysis were performed by the NIH ImageJ software. Approximately 100 cells were measured for each set of experiments and the data are expressed as mean  $\pm$  SEM.

## Results

### Nucleic acid modification of double-stranded probes

In order to optimize the probe for intracellular RNA detection in living cells, we first studied the signal-to-noise ratio of double-stranded probes with alternating DNA/LNA, 2'-O-methyl RNA, and DNA bases targeting  $\beta$ -actin, HO-1, and random sequences.  $\beta$ -actin mRNA, which is a housekeeping gene, has a large number of copies in the cell, and therefore is anticipated to show a high intensity. In contrast, the random probe, with no complementary intracellular mRNA target in the cell, represents the background noise inherent to the assay. The intensities of the probes in the cytoplasm are presented in Figure 2. Figure 3 shows images of cells transfected with dsLNA probes for intracellular mRNA detection in the cytoplasm. The dsLNA probe with alternating DNA/LNA monomers displayed signal-to-noise ratios over 8:1 and 4:1 for detecting  $\beta$ -actin and HO-1 mRNA relative to the control. By comparison, the probe with 2'-O methyl RNA modification showed a lower signal-to-noise ratio (less than 2), while the DNA probe had the lowest signal-to-noise ratio of  $\sim 1.4$  (Figure 2b-c). The low signal-to-noise ratios of 2'-O methyl RNA and DNA probes are possibly due to the non-specific binding of probes and nuclease degradation.<sup>17, 33</sup> The data show that the probe with alternating DNA/LNA monomer has the highest signal-to-noise ratio. The result is consistent with previous data showing the exceptionally high endurance of LNA modified probes and demonstrates the applicability of LNA in double-stranded probes for intracellular detection.<sup>16</sup>

## Intracellular delivery of dsLNA probes

To allow simultaneous detection of a large number of cells, different transfection reagents were evaluated to maximize the transfection efficiency. Figure 4a illustrates the transfection efficiencies achieved using different transfection reagents for delivering the dsLNA probes. Transfection efficiency was measured as the percentage of cells transfected. Lipofectamine gave 35% transfection efficiency while FuGENE HD resulted in 10% transfection efficiency in our experimental condition. Lipofectamine 2000 achieved over 95% transfection efficiency, by far the best of the transfection reagents tested for transfecting dsLNA. In addition to choosing the proper transfection reagent for the study, the optimal reagent-to-probe ratio was also established to maximize the transfection efficiency.<sup>34</sup> We fixed the probe to 1  $\mu\text{g}$  and applied various amounts of Lipofectamine 2000. An optimal value of 2.5  $\mu\text{l}$  Lipofectamine 2000 was observed to achieve 95% transfection efficiency (Figure 4b). Increasing or decreasing this value resulted in a reduction of the transfection efficiency.

Investigation of complex biological systems, such as cell tracking and probing intracellular transportation, can be benefited by selective delivery of molecular probes. For instance, molecular beacons are often delivered to living cells by microinjection. However, the microinjection technique can be invasive, slow, and labor intensive. To address the requirement of single cell delivery, we explored delivery of dsLNA probes by photothermal nanoblade, which has shown to have high efficiency and cell viability.<sup>26, 27</sup> Figure 4c shows delivery of dsLNA probes to single cells selectively. In particular,  $\beta$ -actin probe displayed a high intensity in the cytoplasm compared to the random probe, suggesting specific detection of intracellular mRNA (Figure 4d). In agreement with previous photothermal nanoblade studies, the efficiency for delivering small molecules, e.g., dsLNA, is close to 100%.<sup>26, 27</sup> These results show the robustness of dsLNA using different delivery approaches and demonstrate the applicability of photothermal nanoblade for delivering dsLNA.

## Inducible Gene Detection

Experiments were performed to evaluate the dsLNA probe's ability to detect inducible genes in living cells specifically. Previous reports have shown that treating MDA-MB-231 cells with tBHQ can upregulate heme oxygenase-1 (HO-1) mRNA through the Nrf2 signaling pathway.<sup>28</sup> Figure 5a shows the intensity level of probes inside the cell after 50  $\mu\text{M}$  tBHQ treatment. Data revealed that the  $\beta$ -actin and random probe intensity levels in the cytoplasm remained constant, while the value for the HO-1 probe increased significantly with the addition of tBHQ. An experiment was also designed to detect HSP70 mRNA induced by elevated temperature (Figure 5b). The HSP70 probe intensity increased when the cells were heated at 42°C for 1.5 hours followed by cultured at 37°C for 5 hours post-heating. The intensities for other probes tested remained stable throughout the duration of experiment. These data demonstrate the specificity of the dsLNA probe and verify its ability to detect the expression of inducible genes in living cells.

## Intracellular stability and dynamics of the dsLNA probe

To evaluate the stability and the dynamics of the dsLNA probes in cells, experiments were performed using the donor-quencher (DQ) probe as well as the donor-target (DT) duplex, in which the donor probe was pre-hybridized with the complementary synthetic target prior to transfection to the cells. Figure 6 shows the normalized fluorescent signal of the  $\beta$ -actin and random probes over 4 days. The random DQ probe expressed low fluorescence throughout the duration of the experiment in the cytoplasm (Figure 6a). By comparison, the  $\beta$ -actin DQ probe showed a high signal in the cytoplasm that endured over a long period of time. In particular, the  $\beta$ -actin DQ probe intensity reached a stable value at 12 hours after transfection and remained constant for 60 hours before the intensity gradually decreased. The drop off in the intensity level after 72 hours is possibly due to probe degradation and the dilution effect of cell proliferation. In the nucleus, however, both the  $\beta$ -actin and random DQ probes behaved differently (Figure 6b). For the  $\beta$ -actin probe, the intensity level was maximized at 54 hours while the random probe signal peaked at 12 hours after transfection, suggesting different intracellular dynamics of the specific and non-specific probes. The observed fluorescence of the DQ random probe in the nucleus was significantly elevated compared to its fluorescence in the cytoplasm. This observation suggests that there could be degradation and other molecular interactions of the probe in the nucleus. The data also revealed that the  $\beta$ -actin probe signal reached levels more than double that of the random probe in the nucleus, suggesting that there could be target gene binding in the nucleus. Figure 6c-d shows the DT duplex in the cytoplasm and nucleus. As expected, the pre-hybridized  $\beta$ -actin and random DT duplexes fluoresce at comparable levels, regardless of their presence in the nucleus or cytoplasm. While the relative fluorescence of the DT duplex in the nucleus is more than 3 times higher than in the cytoplasm, the fluorescence intensity of the duplexes increases at similar speeds in both  $\beta$ -actin and random probes. Furthermore, the maximum intensity of both DT duplexes occurred at 12 hours post-transfection in the cytoplasm whereas this peak was observed in the nucleus 24 hours after transfection. Consistence with the DQ data, the results further support a kinetic transition of double-stranded probes from the cytoplasm to the nucleus.

## Quantification of intracellular mRNA

The dsLNA probe concentration in the cells is required to quantify the target concentration based on the equilibrium analysis. To determine the intracellular probe concentration, a serial dilution experiment was performed on cover slips for calibrating the probe intensity. A linear intensity calibration curve is determined to correlate the fluorescence intensity and the probe concentration:  $I = 0.568C + 0.119$ , where  $I$  is the normalized relative intensity and  $C$  is the concentration of the random DT duplex in nM. Based on this linear intensity calibration curve, we estimate the average duplex concentration in the cells was 0.39 nM. Applying this value to our equilibrium analysis method, we obtained a standard curve for quantitative measurements of mRNAs in living cells (Figure 7). It has been reported that there are approximately 1,500 copies of  $\beta$ -actin mRNA in a cell.<sup>35, 36</sup> Using this reference value with its corresponding  $\beta$ -actin probe intensity determined in our experiment, the fraction of target

binding can be correlated to the fluorescence intensity. The average concentration and copy number of mRNA inside the cells can be determined by the fluorescence intensity using the standard curve. As shown in Figure 7, the dsLNA probe has a dynamic range of 2-3 orders of magnitude, which is most sensitive between 1 pM to 1 nM range representing equivalent 5 to 5000 copies of mRNA per cell. For cells treated with and without tBHQ, the normalized intensities of the HO-1 probes were 0.5 and 0.07 respectively, which represented a 9-fold increase in the concentration of HO-1 mRNA from 0.03 nM to 0.26 nM based on the calibration curve. This value is in good agreement with previous measurement by quantitative real-time PCR, which showed an 11-fold concentration increase in HO-1 after tBHQ addition.<sup>28</sup> To further evaluate the calibration curve for quantitative measurement, we estimate the copy number of HSP70 mRNA molecules to 0.01 nM, equivalent to 60 copies of mRNA molecules in a cell. This value is in reasonable agreement to previous report that ~20 copies of HSP70 mRNA exist in HeLa cells measured by gel electrophoresis.<sup>37</sup> Collectively, our results demonstrate the potential of the dsLNA probes for quantitative measurements in living cells.

## Discussion

Developing efficient biosensing approaches for measuring gene expression in individual living cells will have profound impacts on various biomedical applications. This study focuses on the optimization of the double-stranded probe to address several key issues, including specificity, stability, and probe delivery, toward intracellular gene expression detection in living cells. Our data suggest that the dsLNA probes were not only able to detect specific genes inside a cell over time, but also sense intracellular changes in inducible genes due to applied physical or chemical stimuli. In concert with molecular beacon studies,<sup>16, 17, 38</sup> our results suggest the effectiveness of alternating DNA/LNA oligonucleotide backbone in double-stranded probes for providing a high resistance to nuclease digestion as well as protection against non-specific binding, such as single-stranded binding proteins. By incorporating LNA, the signal-to-noise ratio of the probe is significantly improved over DNA and 2'O methyl RNA toward specific detection of targets. Furthermore, the stability of LNA allows intracellular detection with the dsLNA probe for over three days. The long term stability is a critical aspect for studying various complex biological processes, which often last for days. In addition to the stability, the approach for delivering the probes into the cells is another important factor to consider. Using the optimized transfection conditions, 95% of cells can be transfected simultaneously. Furthermore, we demonstrate rapid delivery of dsLNA probe to individual cells by the photothermal nanoblade. Compared to microinjection, transfection with photothermal nanoblade allows rapid delivery with high efficiency and cell viability. These capabilities will enable the dsLNA probe to be applied in a diverse set of applications.

Our results have revealed two fundamental aspects of the dsLNA probe. Firstly, we observed a size dependence on the kinetics of nuclear transportation of the dsLNA probe. The random probe translocated into the nucleus significantly faster than the  $\beta$ -actin probe. This observation can be explained by the

lack of an intracellular complementary target sequence with the random probe, allowing the probe to freely pass into the nucleus through nuclear pore complexes.<sup>39</sup> In comparison, the large  $\beta$ -actin mRNA hybridized with the  $\beta$ -actin probe and kept it in the cytoplasm for an extended period of time before entering into the nucleus. The size dependence was further supported by the experiment where a pre-hybridized DT duplex was transfected into the cells. The DT probes entered the nucleus at the same rate for the  $\beta$ -actin and random probes. The size dependence provides a possible explanation of the stability of the dsLNA probes over molecular beacons, which is generally smaller than the dsLNA probes. In fact, it has been reported that molecular beacons in MDA-MB-231 has a finite life span of ~30 min and conventional molecular beacons are typically stable in cells for less than 24 hours only.<sup>40</sup> Furthermore, our results demonstrate quantitative detection of intracellular mRNA in living cells. Quantitative detection in living cells has not been demonstrated in either molecular beacons or double-stranded probes. Despite the differences in cell types and experimental conditions, our results are in quantitative agreement with other techniques, such as gel electrophoresis and real-time PCR. The ability for quantitative measurement in living cells will enable a new paradigm in quantitative systems biology and dynamic investigation of complex biological systems.

## Conclusion

In summary, this study establishes the double-stranded probes for intercellular gene expression analysis. Our results demonstrate that dsLNA probes can continuously monitor and quantify mRNA in living cells for a period over 3 days. We have also demonstrated quantification of the number of mRNA in viable cells. Overall, the double-stranded molecular probe represents a powerful approach toward the long-term monitoring of intracellular RNA molecules and carries the potential for use in a wide spectrum of biomedical applications in the future.

## Acknowledgements

This work is supported by NIH Director's New Innovator Award (1DP2OD007161-01), and NSF (0900899).

## Notes and references

<sup>a</sup> Department of Aerospace and Mechanical Engineering, The University of Arizona, Tucson, AZ 85721-0119, USA

<sup>b</sup> Biomedical Engineering Interdisciplinary Program, The University of Arizona, Tucson, AZ 85721-0119, USA

<sup>c</sup> Mechanical and Aerospace Engineering, University of California, Los Angeles, Los Angeles, CA 90095-1597, USA

<sup>d</sup> Department of Pathology and Laboratory Medicine, UCLA, Los Angeles, CA, 90095

<sup>e</sup> Department of Pharmacology and Toxicology, The University of Arizona, Tucson, AZ 85721-0119, USA

<sup>f</sup> BIO5 Institute, The University of Arizona, Tucson, AZ 85721-0119, USA

\*Correspondence and request for materials should be addressed to P.K.W. (e-mail: pak@email.arizona.edu; Tel: 520-626-2215; Fax: 520-621-8191; address 1130 N Mountain Ave, Tucson AZ 857211

1. J. M. Ottino, *Nature*, 2004, **427**, 399.

2. V. Lecault, A. K. White, A. Singhal and C. L. Hansen, *Curr Opin Chem Biol*, 2012, **16**, 381-390.
3. K. Taniguchi, T. Kajiyama and H. Kambara, *Nature methods*, 2009, **6**, 503-506.
4. K. Wang, Z. Tang, C. J. Yang, Y. Kim, X. Fang, W. Li, Y. Wu, C. D. Medley, Z. Cao, J. Li, P. Colon, H. Lin and W. Tan, *Angew Chem Int Ed Engl*, 2009, **48**, 856-870.
5. T. H. Wang, Y. H. Peng, C. Y. Zhang, P. K. Wong and C. M. Ho, *Journal of the American Chemical Society*, 2005, **127**, 5354-5359.
6. Y. Kim, D. Sohn and W. Tan, *International journal of clinical and experimental pathology*, 2008, **1**, 105-116.
7. P. J. Santangelo, N. Nitin and G. Bao, *Journal of Biomedical Optics*, 2005, **10**, -.
8. S. Tyagi and F. R. Kramer, *Nature Biotechnology*, 1996, **14**, 303-308.
9. S. A. E. Marras, S. Tyagi and F. R. Kramer, *Clinica Chimica Acta*, 2006, **363**, 48-60.
10. N. Li and P. K. Wong, *Bioanalysis*, 2010, **2**, 1689-1699.
11. A. K. Chen, M. A. Behlke and A. Tsourkas, *Nucleic Acids Res*, 2008, **36**.
12. M. Majlessi, N. C. Nelson and M. M. Becker, *Nucleic Acids Research*, 1998, **26**, 2224-2229.
13. K. Petersen, U. Vogel, E. Rockenbauer, K. V. Nielsen, S. Kolvrå, L. Bolund and B. Nexø, *Molecular and Cellular Probes*, 2004, **18**, 117-122.
14. O. Seitz, *Angewandte Chemie-International Edition*, 2000, **39**, 3249-+.
15. M. A. Campbell and J. Wengel, *Chemical Society Reviews*, 2011, **40**, 5680-5689.
16. Y. R. Wu, C. J. Yang, L. L. Moroz and W. H. Tan, *Analytical Chemistry*, 2008, **80**, 3025-3028.
17. C. J. Yang, L. Wang, Y. R. Wu, Y. M. Kim, C. D. Medley, H. Lin and W. H. Tan, *Nucleic Acids Research*, 2007, **35**, 4030-4041.
18. V. Gidwani, R. Riahi, D. D. Zhang and P. K. Wong, *Analyst*, 2009, **134**, 1675-1681.
19. Q. Q. Li, G. Y. Luan, Q. P. Guo and J. X. Liang, *Nucleic Acids Research*, 2002, **30**.
20. R. Riahi, K. E. Mach, R. Mohan, J. C. Liao and P. K. Wong, *Analytical Chemistry*, 2011, **83**, 6349-6354.
21. L. E. Morrison, T. C. Halder and L. M. Stols, *Anal Biochem*, 1989, **183**, 231-244.
22. D. Meserve, Z. H. Wang, D. D. Zhang and P. K. Wong, *Analyst*, 2008, **133**, 1013-1019.
23. Z. Wang, V. Gidwani, D. D. Zhang and P. K. Wong, *Analyst*, 2008, **133**, 998-1000.
24. Z. Wang, V. Gidwani, Z. Sun, D. D. Zhang and P. K. Wong, *Journal of Association for Laboratory Automation*, 2008, **13**, 243-248.
25. D. Meserve, Z. Wang, D. D. Zhang and P. K. Wong, *Analyst*, 2008, **133**, 1013-1019.
26. T. H. Wu, T. Teslaa, M. A. Teitell and P. Y. Chiou, *Optics Express*, 2010, **18**, 23153-23160.
27. T. H. Wu, T. Teslaa, S. Kalim, C. T. French, S. Moghadam, R. Wall, J. F. Miller, O. N. Witte, M. A. Teitell and P. Y. Chiou, *Analytical Chemistry*, 2011, **83**, 1321-1327.
28. X. J. Wang and D. D. Zhang, *Plos One*, 2009, **4**.
29. S. Wang, K. R. Diller and S. J. Aggarwal, *J Biomech Eng*, 2003, **125**, 794-797.
30. M. G. Mendez, S. Kojima and R. D. Goldman, *FASEB J*, 2010, **24**, 1838-1851.
31. A. A. Adams, P. I. Okagbare, J. Feng, M. L. Hupert, D. Patterson, J. Gottert, R. L. McCarley, D. Nikitopoulos, M. C. Murphy and S. A. Soper, *J Am Chem Soc*, 2008, **130**, 8633-8641.
32. M. Zuker, *Nucleic Acids Res*, 2003, **31**, 3406-3415.
33. C. Molenaar, S. A. Marras, J. C. M. Slat, J. C. Truffert, M. Lemaitre, A. K. Raap, R. W. Dirks and H. J. Tanke, *Nucleic Acids Res*, 2001, **29**, art. no.-e89.
34. B. Dalby, S. Cates, A. Harris, E. C. Ohki, M. L. Tilkins, P. J. Price and V. C. Ciccarone, *Methods*, 2004, **33**, 95-103.
35. T. Osada, H. Uehara, H. Kim and A. Ikai, *J Nanobiotechnology*, 2003, **1**, 2.
36. H. Bjarnadottir and J. J. Jonsson, *J Biotechnol*, 2005, **117**, 173-182.
37. B. J. Wu, H. C. Hurst, N. C. Jones and R. I. Morimoto, *Molecular and Cellular Biology*, 1986, **6**, 2994-2999.
38. L. Wang, C. Y. J. Yang, C. D. Medley, S. A. Benner and W. H. Tan, *Journal of the American Chemical Society*, 2005, **127**, 15664-15665.
39. L. J. Terry, E. B. Shows and S. R. Went, *Science*, 2007, **318**, 1412-1416.
40. C. D. Medley, T. J. Drake, J. M. Tomasini, R. J. Rogers and W. Tan, *Anal Chem*, 2005, **77**, 4713-4718.

Figure Legends

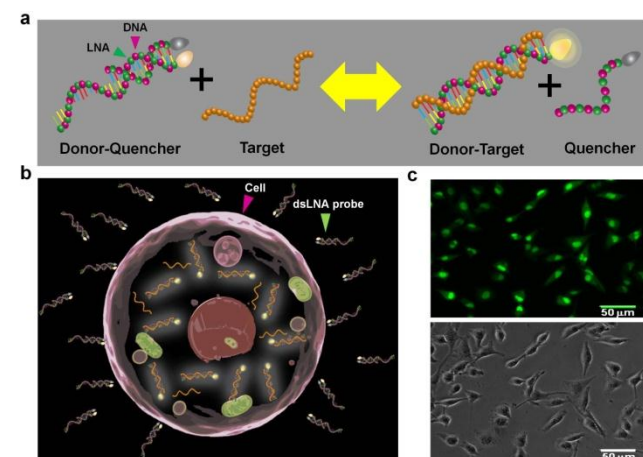


Figure 1. Intracellular gene expression analysis with dsLNA. (a) The homogenous binding scheme of dsLNA for detecting intracellular mRNA. (b) The configuration of dsLNA probes inside and outside of a cell. (c) Fluorescence and bright-field images of MDA-MB-231 cells transfected with dsLNA probes targeting β-actin RNA.

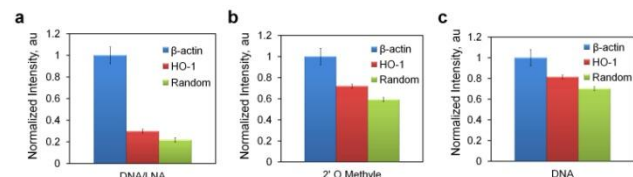


Figure 2. Normalized fluorescence intensity changes of β-actin, HO-1, and random (negative) genes in cell cytoplasm using different monomer modifications. (a) Alternating DNA/LNA, (b) 2'-O-methyl, and (c) DNA.

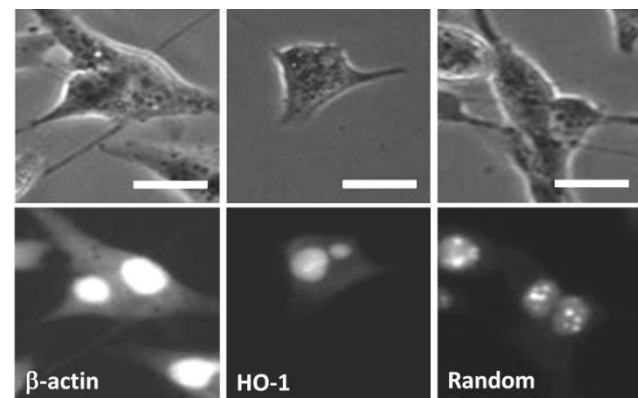


Figure 3. Bright-field (top) and fluorescent (bottom) images of intracellular target gene expression with dsLNA probes targeting β-actin, HO-1, and random mRNA sequences. Scale bars, 20 μm.

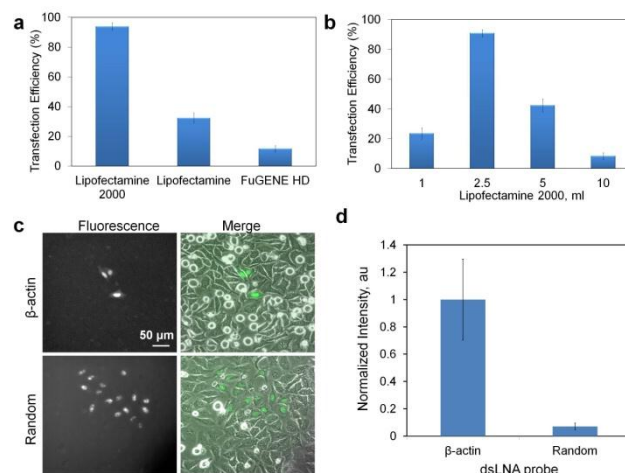


Figure 4. Transfection efficiency of dsLNA probes to cells. (a) Different types of transfection reagent and (b) different amount of lipofectamine 2000 per 1.0 microgram dsLNA probe. (c) Photothermal delivery of dsLNA probes targeting β-actin mRNA and random sequence to HeLa cells.

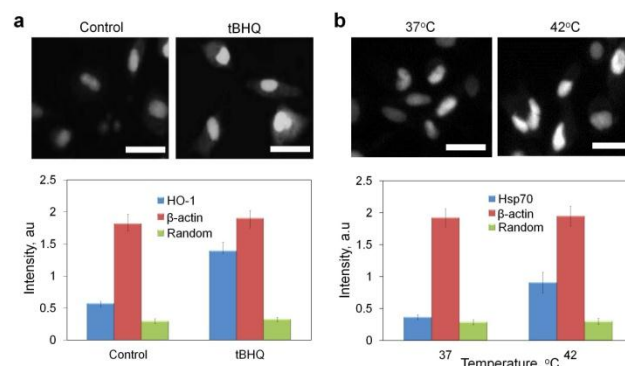


Figure 5. Inducible gene detection with dsLNA probes. (a) Intensity of HO-1 probe in the cytoplasm of the cells treated or untreated with 50 μM tBHQ. (b) Intensity of Hsp70 probe in the cytoplasm of the cells before and after being heated at 42°C. Scale bars, 20 μm.

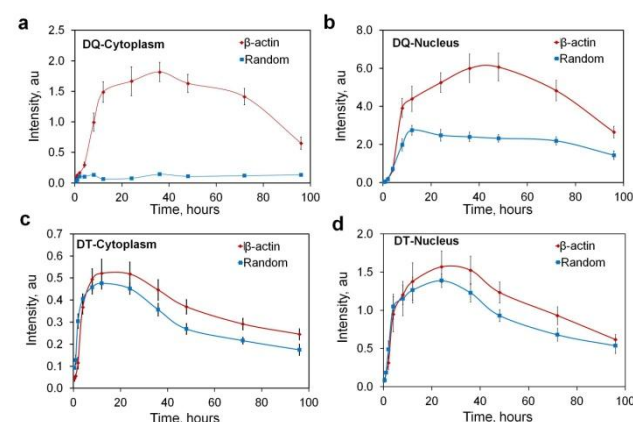


Figure 6. Kinetics of dsLNA probe and its characteristics inside the cell for β-actin mRNA and random sequence. Intensity level of DQ probe and its stability in the cytoplasm (a), and nucleus (b). Intensity level of the donor probe pre-hybridized with synthetic target (DT duplex) in the cytoplasm (c), and nucleus (d).



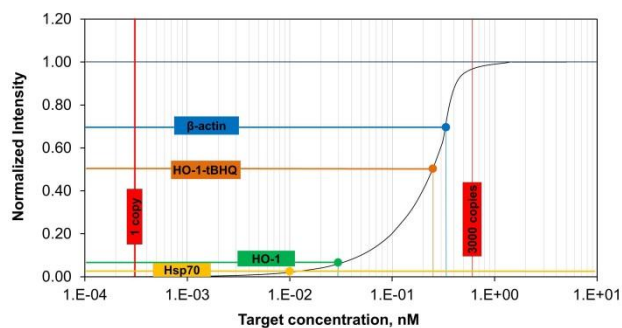


Figure 7. Characteristic calibration curve obtained from the equilibrium analysis with 0.39 nM transfected probe for quantitative measurements on intracellular RNA.  $\beta$ -actin intensity is used as a reference point to normalize the intensity. The intensity values of HO-1 and Hsp70 are indicated in the figure.

Target Gene	Probe Type	Sequence/Label	Length (base)	$\Delta G_{DQ}$ (kcal/mol)	$\Delta G_{DT}$ (kcal/mol)
$\beta$ -actin	Donor (D)	5'- <i><b>FAM-6</b></i> /A GG AA GG AA GG CT GG AA GA G/-3'	20	-10.9	-25.8
	Quencher (Q)	5'-/CTTCCCTCC1/ <i>lowa Black RQ</i> /-3'	10		
	Target (T)	5'-/CTCTCCAG CCTTCCCTCC1/-3'	20		
HO-1	Donor (D)	5'- <i><b>FAM-6</b></i> /A G A C T G G G C T C T C C T T G T /-3'	20	-11.8	-26.6
	Quencher (Q)	5'-/G C C C A G T C T / <i>lowa Black RQ</i> /-3'	10		
	Target (T)	5'/A C A A G G A G A G C C A G T C T /3'	20		
HSP70	Donor (D)	5'- <i><b>FAM-6</b></i> /T T G T C G T G G T G A T G G T G A T /-3'	20	-10.2	-24.9
	Quencher (Q)	5'-/C C A A C G A C A / <i>lowa Black RQ</i> /-3'	10		
	Target (T)	5'-/A T C A C A T C A C C A C G A C A A /-3'	20		
Random	Donor (D)	5'- <i><b>FAM-6</b></i> /A C G C G A C A A G C G C A C C G A T A /-3'	20	-11.1	-26.2
	Quencher (Q)	5'-/C T T G T C G C G T / <i>lowa Black RQ</i> /-3'	10		
	Target (T)	5'/T A T C G G T G C C T T G T C G C G T /3'	20		

Table 1. Sequence of probes with alternating DNA/LNA monomer modification in this study. Bold italic letters indicates LNA monomers. Random sequence is used as a negative control.